

Swell description for Bonga offshore Nigeria location

Akinsanya Akinyemi Olugbenga¹, Ove Tobias Gudmestad^{*1} and Jasper Agbakwuru²

¹Department of Civil, Mechanical and Material Sciences, University of Stavanger, 3056 Stavanger, Norway

²Federal University of Petroleum Resources, FUPRE, Warri, Nigeria

(Received May 27, 2017, Revised October 12, 2017, Accepted November 7, 2017)

Abstract. The ocean environment offshore West Africa is considered to be mild. However, the generated swell from distant North and South Atlantic during austral winter and summer can reach high wave amplitudes with relatively low wave periods or low wave amplitudes with long wave periods, the later can be a crucial scenario to consider when the assessment of vessel resonance is of importance. Most offshore operations, which include offshore drilling, and installation in West Africa, are carried out from floating systems. The response of these systems and performance are governed by characteristics, such as amplitude and frequency of the wave and swell seas. It is therefore important to fully understand the sea conditions offshore Nigeria. This study covers the description of the swell sea offshore Nigeria using Bonga offshore wave measurements collected from the directional wave-rider (DWR), positioned at the Bonga site off the coast of Nigeria.

Keywords: West African swell waves; wave periods; wave heights; extreme value estimates; safe operations of floating vessels

1. Introduction

As there is a growing increase in offshore activities off the West Africa coast, the need to be equipped with good knowledge of swell seas, being dominant, offshore West Africa becomes more important than before, for the planning of successful marine operations in this geographic region. This knowledge is needed to specify the sea states not only for delicate offshore operations (such as drilling) but also for the safe operations of weather sensitive floating vessels in the ocean in this region. It is worthy to note that the knowledge of swell sea is not limited to marine operations; it is also very well applicable for adequate design of offshore facilities specific to this region.

It is known that the ocean environment offshore West Africa is mild, but it is dominated by swell waves, which are generated by high wind energies, far away from offshore West Africa. The waves originate in the South Atlantic and North Atlantic during the austral winter and austral summer, respectively (Prevosto *et al.* 2013). High energies transferred by the wind to the sea results in the propagation of fast moving swell waves, covering enormous distance to West Africa coast. These swells, being generated from sources far from the West African ocean environment, are characterized as low long waves, having long wavelength, with reduced amplitude/wave height, then move further away from the source. However, these swells possess enormous amounts of

*Corresponding author, Professor, E-mail: Ove.t.gudmestad@uis.no

energies transferred by the strong winds at the source, hence making them capable of causing severe impact on sensitive offshore operations and floating constructions, especially on vessels.

Swells in general, and most particularly in this geographical area, have always been the poorly predicted part of the sea states when planning marine operations. Although extensive studies have been performed using both In-situ measurements and Hind cast, to describe and analyze the swells offshore West Africa by several studies and researches such as the West Africa Swell Project of 2004 (Ewans *et al.* 2004). Most of other studies, being carried out on the subject of swells offshore West Africa have been based on the results presented in the WASP final reports (Ewans *et al.* 2004).

This work is intended to add value to the WASP project in the area of development of model prediction tool using available data. The importance of this study cannot be over-emphasized as this work presents a distinctive description of the swell sea states, with short time prediction of the wave heights for marine operations. The Nigeria - Bonga In-situ wave measurements collected from the directional wave-rider, positioned at the Bonga site at the coast of Nigeria (see Fig. 1-1), are used in this analysis.

2. Swell background study

The ocean is a complex and dynamic environment that is characterized not only by the wind waves, which are generated by the local wind, but also by other wave systems, depending on the mode of generation. One of such other types of waves that characterize the ocean environment is the swell. The swell wave is frequently present in every ocean at the same time with the sea waves, and its presence is been felt and recognized across different coasts such as the North Sea, Norwegian Sea and Barents Sea, offshore West Africa, North Indian Ocean, Arabian Sea, Gulf of Mexico, Gulf of Guinea and so on. Empirical data supports the idea that wind seas and swells together account for more than half of the energy carried by all waves on the ocean surface, surpassing the contribution of tides, tsunamis, coastal surges, etc. (Kinsman 1965).

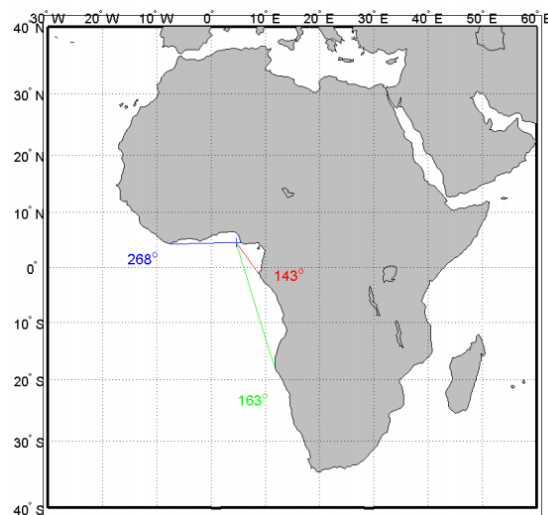


Fig. 1-1 Azimuths from the Bonga Location to Key Land Features (Ewans *et al.* 2004)

Hence the need to fully understand the characteristics of swell was born out of the fact that its existence and characteristics (significant wave height and peak period) affect the description of the ocean surface, which consequently affects marine operations and design through the response of floating constructions.

Generally, the swell waves are being generated by storms at some distance far away from the point of observation. As the wind blows continuously, the sea surface accumulates energy that develops into waves. After the surface has been raised by this storm, long swell waves travel out of this stormy area for thousands of miles, across the entire ocean basin, in the directions of the wind that originated it. The swell waves are characterized by long and regular periods; they travel faster and decay as they advance towards the coast. The reason for the decay is loss of energy due to reduced effect of the storm on the swell as it moves far away from the origin and by friction on the seabed and obstacles in the way. The direction of the waves are affected when they approach the coast, this may be due to the contour of the sea bed, Snodgrass *et al.* (1966), Alves (2006).

It is worthy to note that two or more swell wave systems, originated at different areas, may arrive at the coast, thus making it complex to distinguish the individual wave systems.

A number of various factors determines how big the swell waves will be

- Wind strength/speed.
- Wind duration.
- Fetch length.

Weather systems from different locations, such as North and South Atlantic Ocean, can generate two or more different swell wave trains that independently travel to the coast. In this way, two swell wave trains generated by the separate weather systems can then cross paths at some location. The swell wave trains generated will interact with each other where their paths cross; generating higher peaks where the peaks of the wave trains intersect, and lower troughs where the two troughs meet, but can exist within the same area. Thus, the generated swell trains or components can be categorized as primary and secondary swells, depending on the wave heights, wave period and directions. The primary swell produces the larger wave heights while the second swell train is considered as secondary provided its wave height is significantly smaller than that of the primary and it is propagated from a different direction.

As stated in section 1 swell waves are generated at different locations (see Fig. 2-1) and arrive at various coasts. The subsequent paragraphs describe the swell waves arriving at some different coasts.

Based on National Aeronautical and Space Administration (NASA) satellite sensors, QuikSCAT scatter meters etc., Chen *et al.* (2002) produced global maps of swell climate and based on the study of Alves (2006) three well-defined swell-dominated zones in the tropical areas of Pacific ocean (South and North), Atlantic ocean (South and North), and the Indian ocean were identified, see Fig. 2-1.

The persistent, strong winds over the Southern Ocean near the southern tip of South Africa generate high waves that travel thousands of kilometers to the North Indian Ocean as large swell component with the magnitude of swell height between 15.0 m (near the generation area) and around 6.0 m (near La Reunion island) (Alves 2006). These swells, on entering the Indian Ocean region, contribute to the total wave height of the surface waves. Ardhuin *et al.* (2009) provided an accurate estimation of the dissipation rate of swell energy across the oceans. Study by Bhowmick *et al.* (2011) shows that the Indian Ocean is dominated by swells of considerable amplitudes. These swells arrive from the Southern Ocean during most part of the year and can grow significantly under the influence of strong winds such as storms.

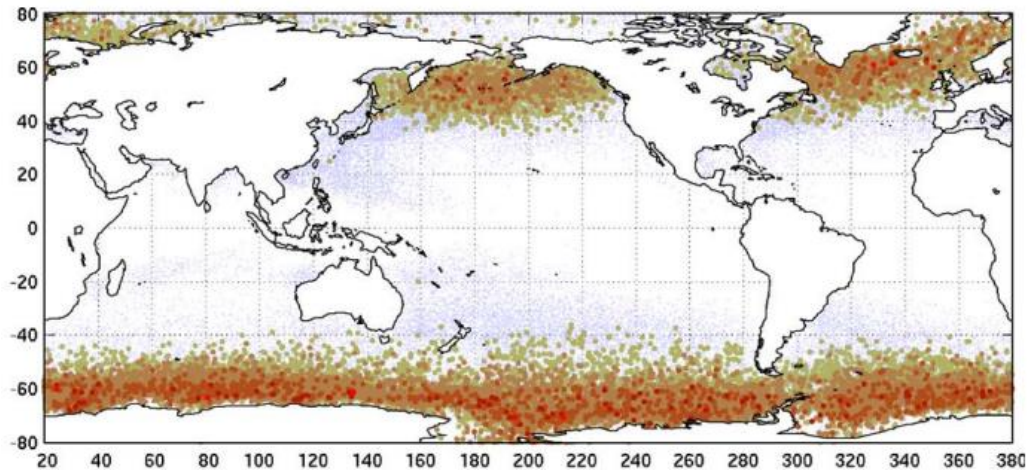


Fig. 2-1 Swell Generation Areas-Storm Extratropical Storm Atlas (Alves 2006)

Bhowmick *et al.* (2011) further identify that the significant wave heights of the swells arriving at the North Indian Ocean are relatively low in the range of 0.5–1 m in the months of April and May. During the months of June to September, the Indian Ocean witnesses swells of larger amplitudes, propagating from the Southern Ocean, and the significant wave height increases to 2.0–3.0 m.

Alves (2006) pointed out that the wave characteristics of the Arabian Sea are less compared to those of the Bay of Bengal when the Atlantic or the South Indian Ocean swells enter the North Indian Ocean.

Most of the long swell waves witnessed on the Norwegian Continental Shelf (NCS) are generated by the intense extratropical cyclones originated in the North Atlantic Ocean, since these seas are at the margin of the Atlantic Ocean. A swell waves have considerable energy at wave periods of 20-25seconds at significant wave heights of 4-5meters (Gjevik *et al.* 1987). Semedo *et al.* (2009) shows that the relatively narrow geometry of the Atlantic Ocean restricts the propagation of Southern Ocean swell waves into the Northern Hemisphere. Therefore the properties and seasonal variation of the swell waves on the NCS are largely determined by the combination of storm frequency, duration, and intensity, and the geographic characteristics of the North Atlantic basin, (Semedo *et al.* 2009)

Prevosto *et al.* (2013) identified that the majority of the swell waves arriving to the offshore West Africa coast are been generated by storms in the South Atlantic ocean and these swells can produce sea-states ranging from 3 meters near the equator to 7 meters offshore South Namibia. Only a few numbers of these swells are generated by North Atlantic storms, with swell significant heights up to 0.5 meters, Prevosto *et al.* (2013). They further established that more frequent swell waves are observed from the Southwest compared to the Northwest.

Past research or studies have been able to cover extensively the description and comparison of the configuration of the swell spectra that are found to be different from both the JONSWAP and PM spectra. It has been identified by Ewans *et al.* (2004), that a double peaked spectrum gives a more detailed and accurate description of the ocean environments off West Africa coast. A log-normal model was recommended for the swell spectra (Ewans *et al.* 2004)

Detailed evaluations of the swell spectral shape were performed by Olagnon *et al.* (2013), by using parametric models that consider each wave system individually (sea and swell waves). The spectra of swell waves offshore West Africa are much narrower both in frequency and in directions than the wind sea spectra that are observed in the North Sea.

2.1 Study limitations

The data available for this study includes monthly and yearly comparison of measured swell significant wave heights. The work targets to identify variability during the season, which can aid accurate short-term prediction as well as determine a model that is best suited for predicting the significant wave height, by fitting the measured H_s to various probability models. The determined model translates to prediction tool for swell significant wave height for weather window required for offshore and marine operational activities in the offshore area under consideration.

The data provided for this study contains only the swell significant wave heights (H_s) and zero-up crossing periods (T_z) corresponding to these H_s . No information was given about the corresponding swell peak periods (T_p). Based on discussion with experts on the subject of wave statistics, since the peak period is always greater than the zero-up crossing period, a factor that ranges between 1.0~1.3, is considered adequate for estimating the T_p from the T_z . *DNV-RP-H103 (2011)* recommends a factor of 1.3 for JONSWAP spectrum and 1.4 for PM spectrum. However, for the case of this study the T_p was determined by conservatively multiplying the T_z by a factor of 1.3. In addition, it was specifically stated for the data received that the directional data look wrong and therefore should not be used.

3. Data discussion and analysis methods

Contrary to a deterministic system whose future state can accurately be determined, the swell wave is a random system since it involves a high level of randomness, thus its future state cannot be easily predicted nor described; even when its present condition is well known.

Hence, its future conditions can only be indicated in terms of probabilities for their various possible outcomes, that is we can only indicate their outcomes by associating probabilities to the various possible outcomes. The accuracy of the prediction depends on the amount of historic data, Haver (2016)

Consequently, since wave loads and the responses of floating structures depend largely on this random system, they are therefore random in nature as well. Thus, because of this random nature of ocean waves, a statistical approach is adopted in order to be able to predict, with a reasonable level of accuracy, the future nature of the ocean waves.

3.1 In-situ measurements

The measured data were taken by a directional wave-rider positioned at Nigeria Bonga site location offshore West Africa, as shown in Figure1-1 and were provided by Shell, Nigeria. Swell data from West Africa have previously been analyzed by Ewans *et al.* (2004). The measured data contain information, such as the sea wave H_s , T_z values and directions as well as the two swell components with H_s , T_z and direction. Relevant to this study is the swell waves significant wave heights, thus the swell wave components' H_s and T_z only are considered in this study.

These measurements were taken every 30minutes, thus to fit a probability model to the measured data, the data were averaged every 3hours, this is done by finding the average of every 6 samples of the swell H_s , hence the number of the samples is reduced to 2053.

3.2 Statistical data analysis

One needs to ensure that the variability of the environmental conditions or sea state are properly described and one needs to know how to approach the response problem in order to determine a consistent estimate of loads and responses corresponding to a given exceedance probability (Haver 2013).

Hence, for the purpose of short-term prediction for marine operations, the significant wave height (H_s) for swell component_1, being the primary swell, is fitted to two probability models. The models considered in this study are the Log-normal and the 3-parameter Weibull. These probability models were considered adequate to predict the swell H_s with a reasonable level of accuracy.

3.2.1 Theory

The first step is to arrange the values of swell H_s in increasing order $\{H_{s_1} < H_{s_2} < H_{s_3} < \dots < H_{s_k}\}$, where k is the total number of H_s samples in the measurements. Then the average significant swell wave height, m_{H_s} , the sample variance, $S_{H_s}^2$ and the coefficient of skewness, g_1 are determined using equations 1 to 3 respectively

$$m_{H_s} = \frac{1}{k} \sum_{i=1}^k H_{s_i} \quad (1)$$

$$S_{H_s}^2 = \frac{1}{k-1} \sum_{i=1}^k (H_{s_i} - m_{H_s})^2 \quad (2)$$

$$g_1 = \frac{\frac{1}{k} \sum_{k=1}^k (h_{s_k} - m_{H_s})^3}{(S_{H_s}^2)^{\frac{3}{2}}} \quad (3)$$

3.2.2 Parameter estimation

There are different approaches to estimating the parameters of any probability distribution function, such as the least square approach, maximum likelihood approach and the method of moments. The method of moment is considered adequate in this study; this is because It gives more weight to the tail and is easy to implement, Haver (2013). This method is adopted for calculating the parameters of the both the Weibull and Lognormal distribution functions as shown below.

3.2.2.1 3-Parameter weibull

Since it is easier to estimate the parameters of the 3-parameter Weibull distribution and if one is not too concerned regarding non-exceeding parameters for significant wave close to the 3rd parameter (location parameter, λ), a 3-parameter Weibull is recommended Haver (2013).

The expression for the distribution of the 3-parameter Weibull distribution is given as

$$F_{H_s}(h) = 1 - \exp \left[- \left(\frac{h - \lambda}{\alpha} \right)^\beta \right] \quad (4)$$

Where the parameters of the distribution are determined using the *method of moments* and the following equations are adopted for estimating these parameters.

a) Shape Parameter, β ; γ (the Gamma function)

$$\gamma_1 = \frac{\gamma \left(1 + \frac{3}{\beta} \right) - 3\gamma \left(1 + \frac{1}{\beta} \right) \gamma \left(1 + \frac{2}{\beta} \right) + 2\gamma^3 \left(1 + \frac{1}{\beta} \right)}{\left[\gamma \left(1 + \frac{2}{\beta} \right) - \gamma^2 \left(1 + \frac{1}{\beta} \right) \right]^{\frac{3}{2}}} \quad (5)$$

By requiring $\gamma_1 = g_1$, the shape parameter, β , can be estimated from Eq. (5) by a simple iteration process.

b) Scale Parameter, α ;

Introducing this estimate for β into Eq. (6) below, and requiring $\sigma_{H_s}^2 = s_{H_s}^2$, the scale parameter, α , is estimated.

$$\sigma_{H_s}^2 = \alpha^2 \left[\gamma \left(1 + \frac{2}{\beta} \right) - \gamma^2 \left(1 + \frac{1}{\beta} \right) \right] \quad (6)$$

c) Location Parameter, λ ;

Finally, the location parameter, λ , is estimated from Eq. (7) by requiring $\mu_{H_s} = m_{H_s}$

$$\mu_{H_s} = \lambda + \alpha \gamma \left(1 + \frac{1}{\beta} \right) \quad (7)$$

These parameters are found by solving the above equations and the results are presented in Table 1-1.

3.2.2.2 Log-normal

One could also obtain an equally good fit (possibly better for very low sea states) using an hybrid model, i.e. log-normal distribution for $h_s \leq \eta$ and a 2-parameter Weibull distribution for $h_s > \eta$, Haver and Nyhus (1986). If one primary concern is with significant wave height less than about 1m, one should possibly just fit a log-normal distribution to the measurements Haver (2013).

The expression for the Log-normal Distribution is given as

$$F_{H_s}(h) = \frac{1}{2} \operatorname{erfc} \left[- \frac{\ln h - \mu}{\sigma \sqrt{2}} \right] = \Phi \left(\frac{\ln h - \mu}{\sigma} \right) \quad (8)$$

Where the erfc is a complementary error function and Φ is the cumulative distribution function of the standard normal distribution.

The two parameters are estimated using the method of moments

d) Scale parameter, μ

The scale parameter is estimated using Eq. (9), Ginos (2009)

$$\mu = -\frac{\ln\left(\sum_{i=1}^k Hs_i^2\right)}{2} + 2\ln\left(\sum_{i=1}^k Hs_i\right) - \frac{3}{2}\ln(k) \quad (9)$$

e) Location Parameter, σ^2

The location parameter is estimated using Eq. (10), Ginos (2009).

$$\sigma^2 = \ln\left(\sum_{i=1}^k Hs_i^2\right) - 2\ln\left(\sum_{i=1}^k Hs_i\right) + \ln(k) \quad (10)$$

These parameters are found by solving the above equations using MATLAB and the MATLAB results are presented in table 1-2 in chapter 4.

3.3 Plotting on probability paper

One way to get an early indication of whether the probability model can reasonably predict the variable, in this case the swell wave H_s , is to plot the data assuming an empirical distribution function in a probability paper. If the plot looks like it could be a straight line, the model assumption is to a certain extent supported (Haver 2013). Hence, the data are plotted separately on probability paper assuming two-probability model, followed by a comparison with an empirical distribution.

The first step in achieving this goal is to arrange the values of swell waves H_s in an increasing order such as $\{H_{s_1} < H_{s_2} < H_{s_3} < \dots < H_{s_k}\}$, where k is the total number of H_s samples in the measurements. Afterwards, the distribution functions are linearized as follows;

3-parameter Weibull;

From Eq. (4) above, the Weibull distribution function is linearized as

$$\ln(-\ln(F_{H_s}(h))) = \beta \ln(h - \lambda) - \beta \ln \alpha \quad (11)$$

Hence, for the empirical distribution we will consider a plot of

$$\beta \ln(h - \lambda) - \beta \ln \alpha \text{ vs } \ln(h - \lambda)$$

And for the fitted distribution a plot of

$$\ln(-\ln(F_{H_s}(h_k))) \text{ vs } \ln(h - \lambda)$$

Where $F_{H_s}(h_k)$ is as given in Eq. (12).

$$F_{H_s}(h_k) = \frac{k}{n+1}; \quad k = 1,2,3, \dots, n \tag{12}$$

Hence we will consider a plot of

Log-normal;

From Eq. (8) above, the Log-normal distribution function is linearized as

$$[-erfc^{-1}(2F_{H_s}(h_k))] = \left[\frac{\ln h}{\sigma\sqrt{2}} - \frac{\mu}{\sigma\sqrt{2}} \right] \tag{13}$$

Hence, the plot to be considered for the empirical distribution is give as

$$\left[\frac{\ln h}{\sigma\sqrt{2}} - \frac{\mu}{\sigma\sqrt{2}} \right] \quad vs \quad \ln[h_k]$$

For $k = 1, 2, 3, 4, \dots, n$

While for the fitted distribution, the plot to be considered is given as

$$[-erfc^{-1}(2F_{H_s}(h_k))] \quad vs \quad \ln[h_k]$$

Where $F_{H_s}(h_k)$ is as given in Eq. (12).

3.4 Significant wave height prediction

The expression for short and long term prediction of the significant wave height of the swell waves for the two probability models are derived below.

3-parameter Weibull

From Eq. (4),

$$F_{H_s}(h_y > h) = \exp \left[- \left(\frac{h - \lambda}{\alpha} \right)^\beta \right] = \left(\frac{1}{n_{3h}} \right)$$

$$\ln(-\ln(F_{H_s}(h))) = \beta \ln(h - \lambda) - \beta \ln \alpha$$

$$\frac{1}{\beta} \ln(-\ln(F_{H_s}(h))) + \ln \alpha = \ln(h - \lambda)$$

$$\exp \left[\frac{1}{\beta} \ln(-\ln(F_{H_s}(h))) + \ln \alpha \right] + \lambda = h \tag{14}$$

Log-normal

From Eq. (8),

$$F_{H_s}(h_y > h) = 1 - \frac{1}{2} \operatorname{erfc} \left[-\frac{\ln h - \mu}{\sigma\sqrt{2}} \right] = \left(\frac{1}{n_{3h}} \right)$$

$$\left[-\sigma\sqrt{2}(\operatorname{erfc}^{-1}(2(1 - F_{H_s}(h)))) \right] = \ln h - \mu$$

$$\exp \left[-\sigma\sqrt{2}(\operatorname{erfc}^{-1}(2(1 - F_{H_s}(h)))) + \mu \right] = h$$

In both cases of the probability model the annual exceedence probability F_{H_s} is given as

$$F_{H_s}(h) = \left(\frac{1}{n_{3h}} \right) \quad (15)$$

4. Methods of data analysis

The focus of this study will be on the swell sea states. Thus, the swell data description in this section will only include the description of the two swells components at the Bonga site offshore Nigeria.

4.1 Probability model parameter estimations

The parameters of the probability models for the two swell components are calculated and tabulated in Tables 1-1 and 1-2. The expressions for estimating these parameters follow the explanation in Chapter 2.

Table 1-1 Values of the 3 parameters of the weibull model

Swell Wave Components	m_{H_s}	$s_{H_s}^2$	g_1	β	α	λ	k
1	0.7561	0.0959	0.7577	1.8261	0.6141	0.2103	2053
2	0.7228	0.0428	1.0739	1.4984	0.3371	0.4184	

Table 1-2 Values of the 2 parameters of the log-normal model

Swell Wave Components	μ	σ	k
1	-0.3571	0.3937	2053
2	-0.3640	0.2805	

4.2 Seasonal/monthly comparison

As the data provided are discontinuous, a comparison of the swell significant wave height was made between the month common to both years, which are July 1998 and 1999 where the data was available.

4.2.1 Significant Wave Heights

Figs. 4-1 and 4-2 show the plots of swell significant wave heights for the month of July for years 1998 and 1999, for the two swell components arriving at the coast of West Africa.

There are two swell wave components arriving at the Bonga site offshore Nigeria. These are swell wave component-1 and component-2. Swell wave component-1 are swell waves generated by storms in the South Atlantic. This component-1 is characterized by swell waves with T_z ranging between 12.8 ~ 20.0 seconds. The swell wave component-2 are swell waves generated by storms in the North Atlantic, this component-2 is characterized by swell waves with T_z ranging from 9.0 ~ 12.2 seconds.

It is observed that in general, there is a relatively strong difference between the measurements of H_s recorded in July of the two years, for the two components of swell waves. The reason for this behavior can be well understood by a close study of the ocean environment at the source location.

One should most likely expect the time history of the swell wave H_s system to assume different values every season or month of the year.

The pattern the time history of the swell waves H_s follows is largely dependent on the ocean environment at the source location, most especially dependent on the magnitude of storm and fetch length at the source. The use of two years of data to draw conclusions about the swell condition might furthermore not be reasonable.

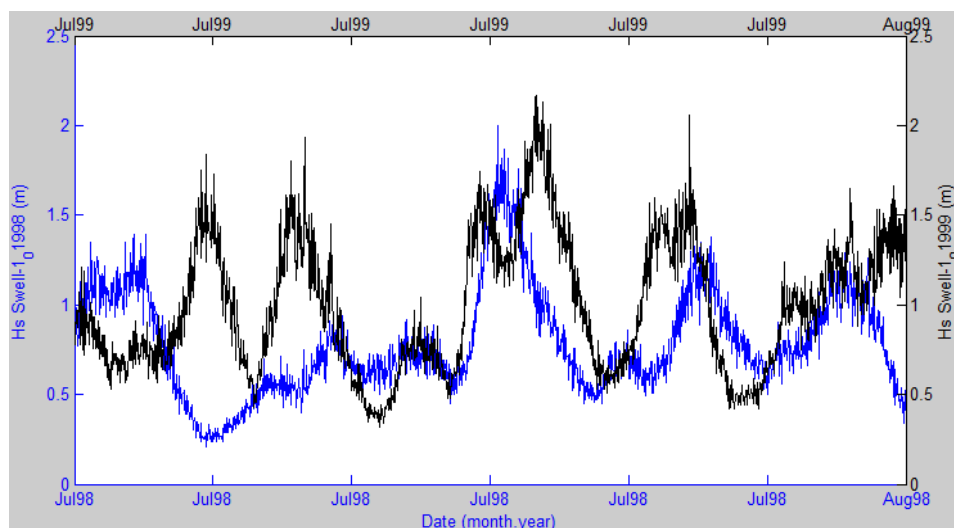


Fig. 4-1 H_s Time History for July 1998 and 1999 Swell component-1

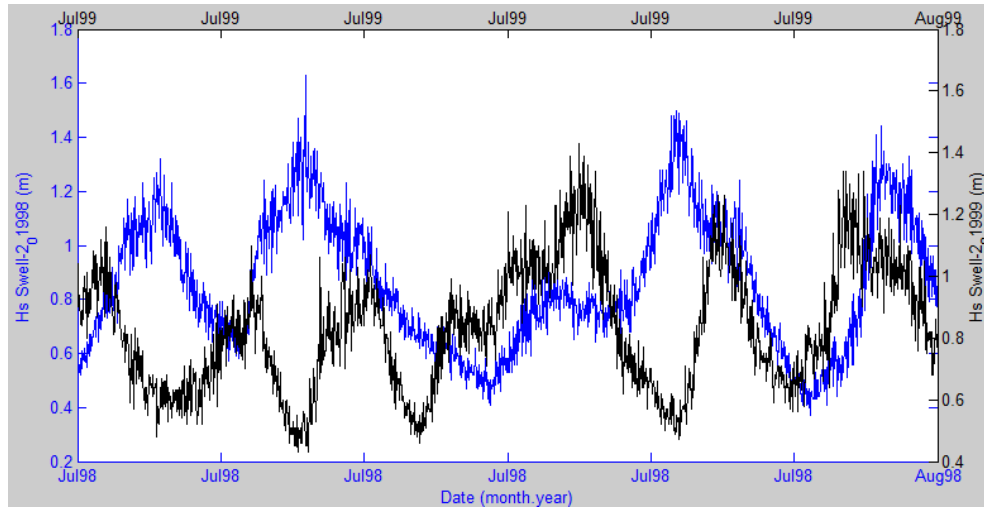


Fig. 4-2 Hs Time History for July 1998 and 1999 Swell component-2

4.2.2 Peak period

Contrary to the swell wave Hs, the peak period (T_p) or mean zero-up crossing periods (T_z) for both years in the month of July, generally agrees well and the time history roughly follows the same pattern, Fig. 4-3. It is observed that the values of T_z or T_p are occurring with nearly the same magnitude, this is a good coincidence.

It should also be noticed that the peak period of swell component_2 is significantly lower than for component_1, as shown in Fig. 4-4.

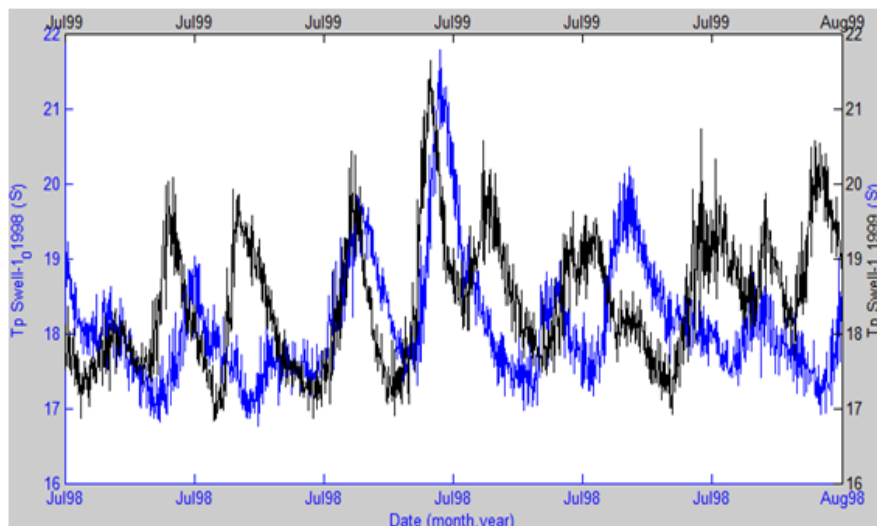


Fig. 4-3 T_p Time History for July 1998 and 1999 Swell component-1

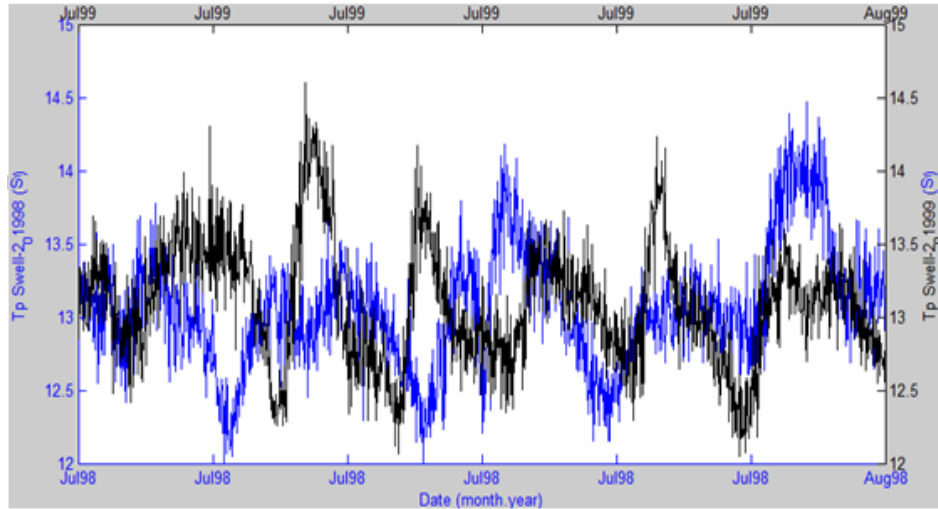


Fig. 4-4 Tp Time History for July 1998 and 1999 Swell component-2

It also follows from the Hs and Tp scatter plots (see Figs. 4-5 and 4-6) that the distributions of the sea states, in terms of swell waves, fall within a certain range. This range may differ depending on the month of the year. Hence, sea states predictions for a particular month or season can be made using a monthly or seasonal range.

Hence, it can be deduced that the sea states for any month or season will fall within the range of the distribution for that corresponding month, as shown for the case of July.

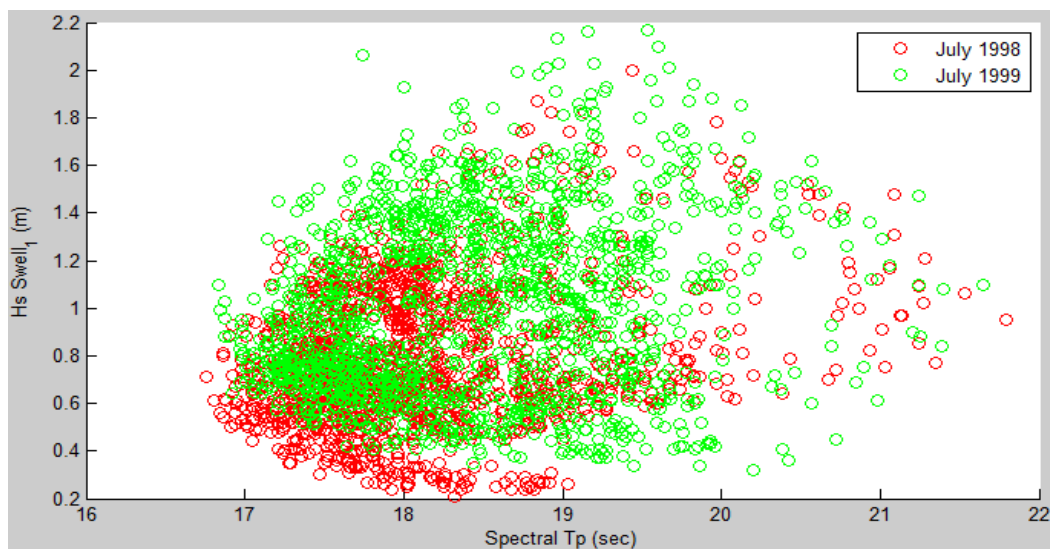


Fig. 4-5 Hs and Tp Scatter Plot for July 1998 and 1999- Swell component-1

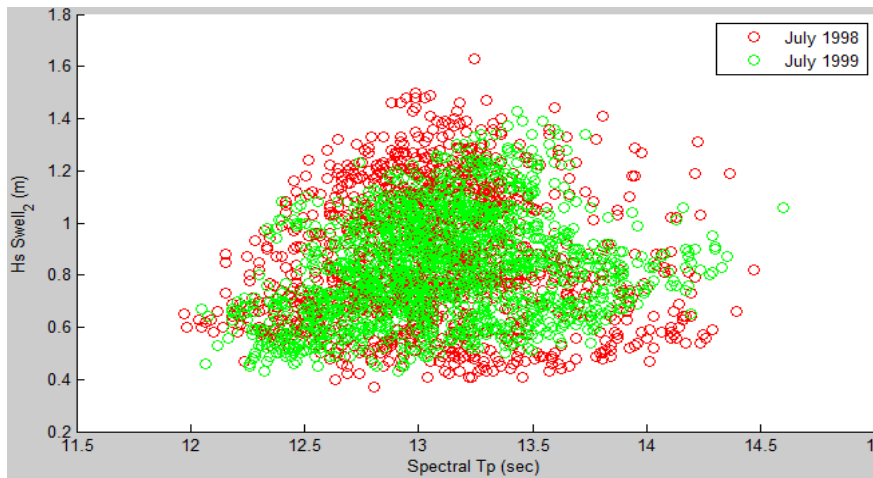


Fig. 4-6 Hs and Tp Scatter Plot for July 1998 and 1999- Swell component-2

4.3 Yearly comparison

4.3.1 Significant swell height, Hs

Fig. 4-7 below shows the time history of the swell wave Hs for the two swell components. It is observed that the Hs for swell component-1, is higher than the Hs of component-2 for the duration when the measurements were taken (the maximum Hs recorded by the wave-rider for component-1 is 2.17 m while component-2 is 1.92 m). Although the duration of the available in-situ measurements might seem insufficient to make long-term predictions, a lower and upper bound of the swell Hs can be established, for both swell components, from this time history for short-term prediction for use in planning of marine operations.

It should be noted that, for marine operations and for the responses of floating construction vessels off the West African coast, close attention should be paid to resonance with the vessels Eigen-periods because of the presence of swell waves with long periods, as seen in the scatter plot.

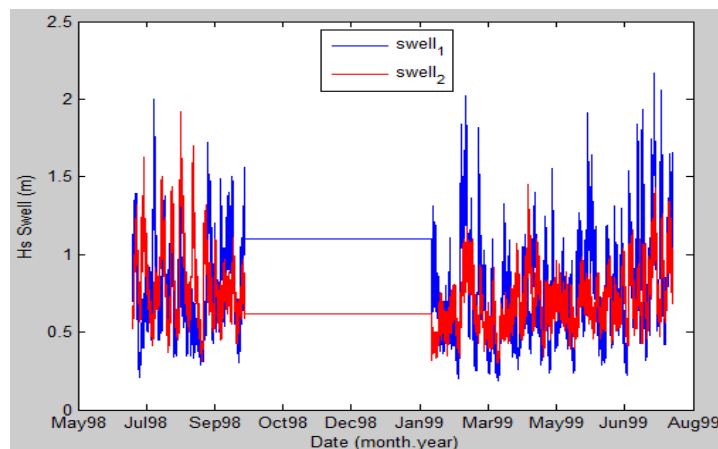


Fig. 4-7 Hs Time History of swell components 1 & 2

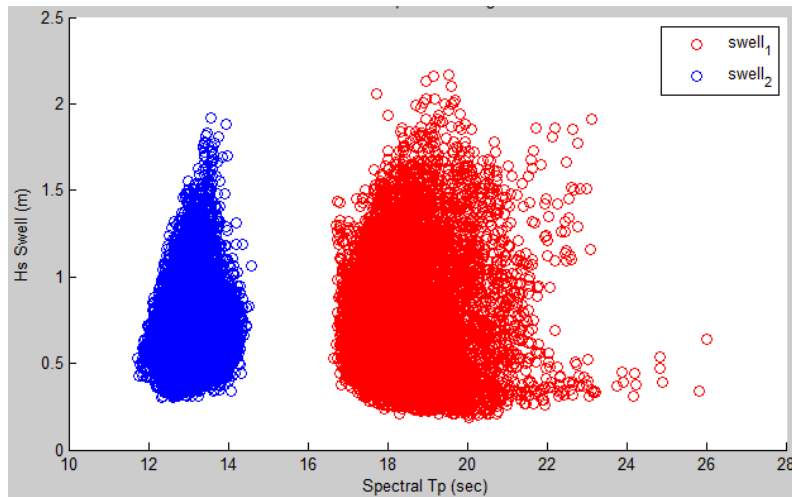


Fig. 4-8 Hs and Tp scatter Plot of swell components 1 & 2- including all data available

4.3.2 Periods

The scatter plots of the Hs and Tp for the two swell components clearly indicates that, the two swell components belong to two different swell systems, with the swell component_1 having the larger Tp. Hence, it is very clear that the two swell components are generated by two different ocean conditions at the source.

It is also observed that in general, the sea states (Hs and Tp) for the two components fall within defined boundaries, as shown Figure 4-8. With component-1, covering more distributed area and component-2 fully concentrated within the bound. Because of this scatter plot, a reasonable 1-2years sea state prediction can be made, most especially for the primary swell. It should be noted that swell component 1 have spectral high peak periods. From Fig. 4-8, we can read that spectral peak periods can be close to 24 seconds, even for significant wave heights close to 2m. Based on the values of Hs and Tp for the swell wave components as shown in the Fig. 4-8, it can be deduced that swell component-1 is the primary swell while swell component-2 is a secondary swell.

5. Data analysis and predictions

The measured data are fitted to two different probability models as mentioned previously. The results of considering the plots on probability paper in order to identify the most suitable model are presented in this section.

5.1 Fitting distributions to data

5.1.1 3-parameter weibull model

Figs. 5-1 and 5-2 below show a comparison of the 3-parameter Weibull distribution with the empirical distribution for the two swell wave components. It is observed that there is good fit correlation between the empirical distributions and the model distributions at the upper tail. This

reveals the adequacy of the 3-parameter Weibull distribution to predict the upper tail of the curve. Since the upper tail is of more concern to us, based on the plots, the 3-parameter Weibull model seems to be the reasonable model for short term predicting of the swell Hs required for marine operations, for the two swell wave components.

It is to note that for a certain number of years, any positive or negative departure from the tail of the fitted distributions, indicates that the significant wave height Hs, will be over or under predicted accordingly by the Weibull probability model. Hence, measured data for a reasonable number of years is required in order to ascertain the suitability of the 3-parameter Weibull model.

The values of the plot functions for different return periods are given in Table 2-1.

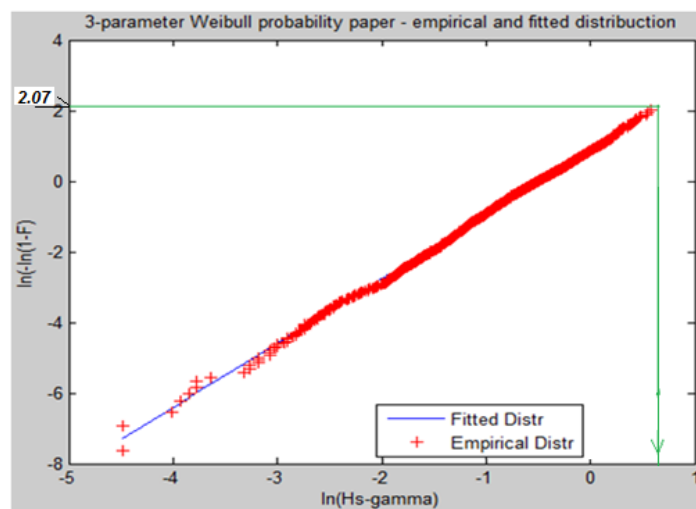


Fig. 5-1 Empirical and fitted 3-parameter Weibull Distr. for the Component-1 Swell Hs

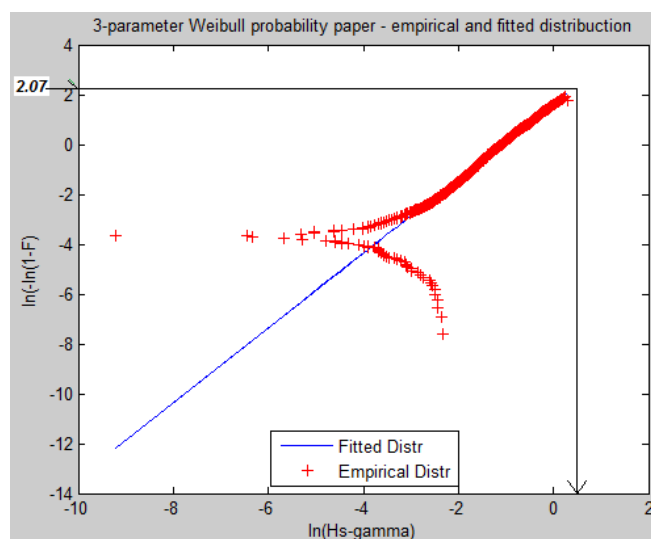


Fig. 5-2 Empirical and fitted 3-parameter Weibull Distr. for the Component-2 Swell Hs

Table 2-1 Plot Function Values of 3-parameter Weibull Distr. for Swell Components Hs for Different

Return Period (years)	n_{3h}	$\ln(-\ln(1-F))$ Components 1 & 2 Swell
1	2920	2.07
10	29200	2.33
100	292000	2.53

5.1.2 Log-normal model

The Log-normal distributions (see Table 2-2) were used to fit the two swell wave components, adopting the standard deviation of the Hs in-situ measurements, as shown in Figs. 5-3 and 5-4. By comparing this with the empirical distributions it is observed, that the sample distributions are closely fitted at the middle part, however there are departures at the two tails, both positive and negative as shown. This indicates the inadequacy of the log-normal model to predict the upper tail of the curve, as it grossly over-predicts and under-predicts the significant wave height in the case of swell components 1 and 2 respectively (see Figs. 5-3 and 5-4). For component-2, based on Fig. 5-4, there is an uncertainty about the behavior of the empirical distribution at the upper tail of the curve, thus it cannot be deduced with certainty that the Log-normal distribution will grossly under-predicts the Hs (see Fig. 5-4 for 1-year return period prediction). In order to reduce the uncertainty and establish the behavior at the upper tail, more measured swell significant wave heights samples may be required.

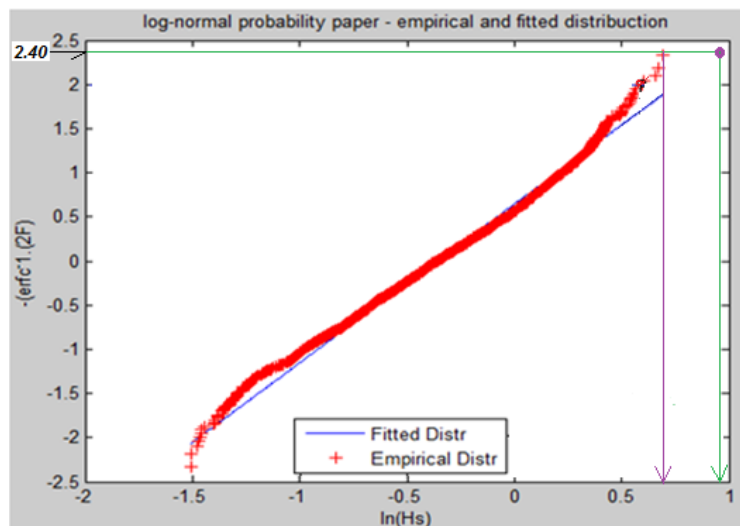


Fig. 5-3 Empirical and fitted Log-normal distribution for the Component-1 Swell Hs

Table 2-2 Plot Function Values of Log-Normal Distr. for Swell Components 1 & 2 Hs for Different Return Periods

Return Period (years)	n_{3h}	$\text{Erfc}^{-1}(2*F)$ Components 1 & 2 Swell
1	2920	2.40
10	29200	2.82
100	292000	3.18

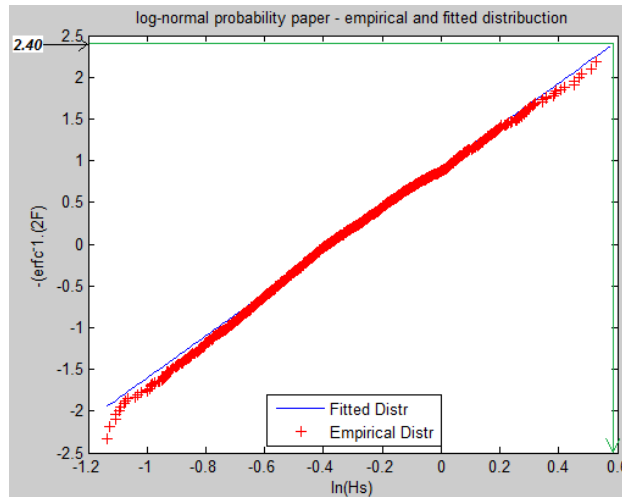


Fig. 5-4 Empirical and fitted Log-normal distribution for the Component-2 Swell Hs

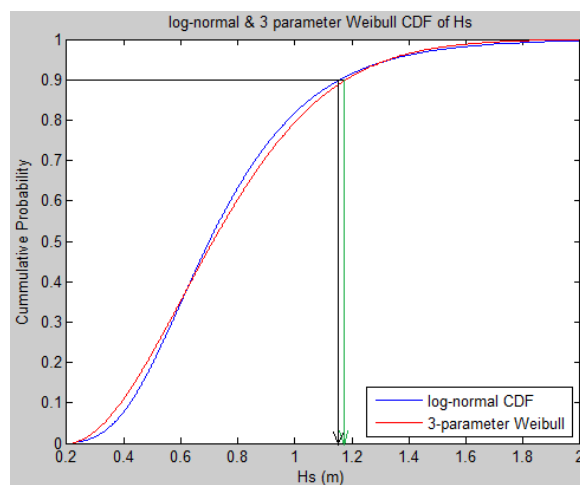


Fig. 5-5 3-parameter Weibull & Log-normal Probability Density Functions – Component-1

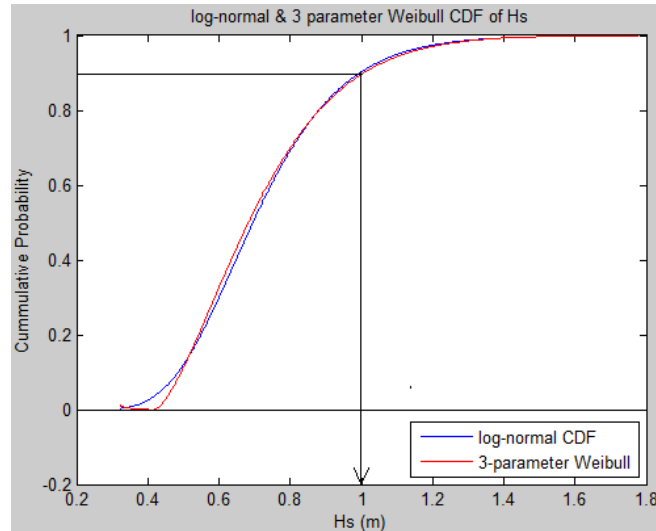


Fig. 5-6 3-parameter Weibull & Log-normal Probability Density Functions – Component-2

Following these plots (Figs. 5-1 to 5-4), it may not be reasonable to adopt the Log-normal model to predict the upper end of the curve i.e. the H_s , as it can give only an indicative level of accuracy. However, the 3-parameter Weibull will give a more accurate prediction than the Log-normal. Hence, the 3-parameter Weibull is recommended for prediction of the swell H_s .

5.1.3 CDF of the probability models

For each of the two swell wave components, the cumulative distributions (CFD) for the two models are as shown Figs. 5-5 and 5-6. The CDF plots show that there is no significant disparity between the values of swell H_s obtained from the two models for normal operational probability (see Figs. 5-5 and 5-6 for CDF of 0.9).

5.2 1-year significant wave height prediction

For short term prediction, a 1-year return period will be considered in this study refer to DNV. The expression for predicting the swell significant wave height is derived in section 2.4. For a 1-year return period, the number of samples n_{3h} , is estimated as

$$n_{3h} = (24/3) \times 365 = 2920$$

Hence, from Eq. (15), the probability of exceedance is estimated as

$$F_{H_s}(h) = 3.425 \times 10^{-4}$$

The parameters are given as in Table 2-3;

Following the argument that the 3-parameter Weibull distribution is best to predict the upper tail of the curve, a comparison between the in-situ measured H_s and the estimated H_s as shown in Table 2-3, further confirms the accuracy of the 3-parameter Weibull model in predicting the swell H_s . For the case of swell component-1, there is a disparity of 0.13 m between the maximum measured H_s of the averaged samples recorded by the wave rider at the Bonga site during 1998

and 1999 and the 1-year estimated Hs, with the estimated value higher, this will be expected difference between short term measurements and modeling the measured data.

It should be noted that the differences between the estimated and measured significant wave heights for the two swell wave components (0.13 m and 0.01 m respectively) are small and can be considered negligible for practical purposes.

It should be observed that the Log-normal model can also give a reasonable level of accuracy for short term predictions. The estimated swell Hs in Table 2-4 is reasonably close to the measured value, this also validate the Log-normal fitted curve in Fig. 5-4.

5.3 Extreme 100-year significant wave height

For the extreme value prediction, a 100-year return period will be considered in this case for a 100-year return period, the number of samples are

$$n_{3h} = (24/3) \times 365 \times 100 = 292000$$

Thus from equation (15), the probability of exceedance is estimated as

$$F_{H_s}(h) = 3.425 \times 10^{-6}$$

Table 2-3 Max. Hs of the Average Samples & Estimated Hs for 1year return Period

Swell Wave Components	Probability Model	n_{3h}	$F_{H_s}(h)$	Max. Hs of the Averaged Samples	Estimated Hs, Return Period 1 year
1	Weibull	2920	3.425×10^{-4}	2.00	2.13
	Log-normal				2.66
2	Weibull	2920	3.425×10^{-4}	1.78	1.77
	Log-normal				1.80

Table 2-4 Max. Hs of the Average Samples & Estimated Hs for 100years Return Period

Swell Wave Components	Probability Model	n_{3h}	$F_{H_s}(h)$	Max. Hs of the Averaged Samples	Estimated Hs, Return Period 100 years
1	Weibull	292000	3.425×10^{-6}	2.00	2.67
	Log-normal				4.11
2	Weibull	292000	3.425×10^{-6}	1.78	2.25
	Log-normal				2.45

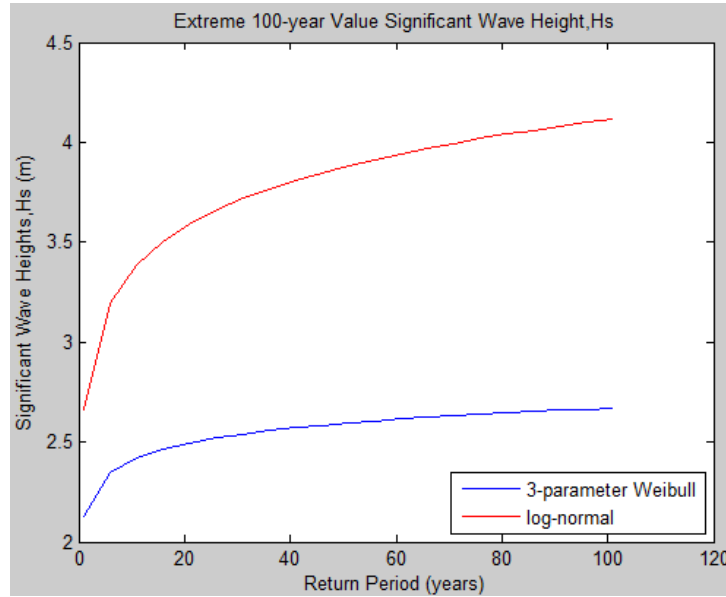


Fig. 5-7 Distribution of Significant Wave Height in Years- Component-1

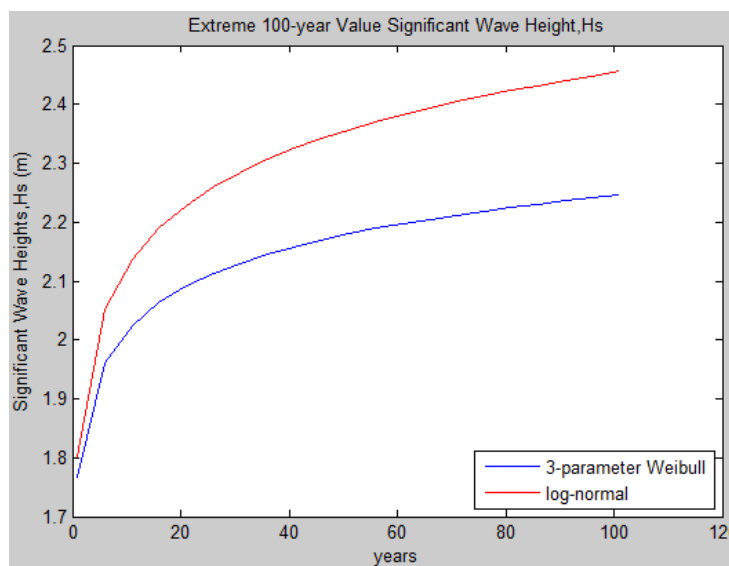


Fig. 5-8 Distribution of Significant Wave Height in Years – Component-2

5.4 Distribution of H_s with return period

Figs. 5-7 and 5-8 show the distribution curves of the swell significant wave height with return period for the two swell components. The Figures show that Log-normal distribution over-predicts the swell significant wave heights for the two components. Hence, it can be deduced that the

over-prediction of H_s occurs from return periods of 1 year and above. This validate the statement made in section 5.1.2, that more measured swell significant wave height samples may be required to establish the behavior of the empirical distribution at the upper tail.

6. Conclusions

There is a reasonable level of variability in the monthly and yearly values of the swell significant wave height and zero-mean crossing period in the data provided. The comparison shows significant disparities in the time histories of the H_s and T_p . The same values of H_s and T_p should not be expected every year; however, there is no significant difference between values of the H_s recorded for the years considered (1998 and 1999).

The results of the analysis show that the 3-parameter Weibull model may be sufficiently accurate for predicting the swell significant wave height, thus it could be adopted for prediction of the swell significant wave height while planning marine operations. For planning marine operations, a 1-year return-period swell wave H_s is considered reasonably adequate as estimated in section 5.2, Table 2-3. Design wave conditions (100-year return period waves are discussed in section 5.3.

Swell components 1 have spectral high peak periods. From Fig. 4-8 we can read that spectral peak periods can be close to 24 seconds, even for significant wave heights close to 2 m.

Future work

A further study when more detailed information is available will be the assessment of the swell sea states, establishment of general weather windows and evaluation of the sensitivity of installation vessels to swell seas offshore West African.

Acknowledgements

Special thanks to Center for Offshore and Maritime Studies unit of the Federal University of Petroleum Resources Effurun (FUPRE), Nigeria and to Shell Nigeria for providing the in-situ measurements used for this study. We also want to thank Adekunle P. Orimolade and Sverre Haver of University of Stavanger for providing various input information on the subject matter, and documentations on past studies related to this present study.

References

- Alves, J.H.G.M. (2006), "Numerical modeling of ocean swell contributions to the global wind wave climate", *Ocean Modell.*, **11**(1-2), 98-122.
- Ardhuin, F., Bertrand, C. and Fabrice, C. (2009), "Observation of swell dissipation across oceans", *Geophys. Res. Lett.*, **39**.
- Bhowmick, S., Kumar, R., Chaudhuri, S. and Sarkar, A. (2011), "Swell propagation over Indian Ocean Region", *Int. J. Ocean Clim. Sys.*, **2**, 87-99.
- Bureau of Meteorology, Australian Govt. (2017), "Second swell", <http://www.bom.gov.au/marine/about/forecast/second-swell.shtml>

- Ginos, B.F. (2009), "Parameter estimation for the lognormal distribution", Brigham Young University. Master of Science Thesis, Department of Statistics, Brigham Young University December.
- Chen, Y.H., Francis, J.A. and Miller, J.R. (2002), "Surface temperature of the arctic: Comparison of TOVS satellite retrievals with surface observations", *J. Climate*, **15**, 10.1175/1520-0442, 3698-3708.
- DNV-RP-H103. (2011), "Modelling and analysis of marine operations, recommended practice", Last Modified April. <https://rules.dnvgl.com/docs/pdf/DNV/codes/docs/2012-12/RP-H103.pdf>.
- Ewans, K., Forristall, G.Z., Olagnon, M., Prevosto, M. and Van Iseghem, S. (2004), "WASP-West Africa Swell Project – Final Report", 90+192. <http://archimer.ifremer.fr/doc/00114/22537/>
- Forristall, G.Z., Ewans, K., Olagnon, M. and Prevosto, M. (2013), "The West Africa Swell Project (Wasp)", *Proceedings of the 32nd Int. Conf. on Offshore and Arctic Eng.*, OMAE 2013-11264.
- Gjevik, B., Krogstad, H.E., Lygre, A. and Rygg, O. (1987), "Long period swell wave events on Norwegian shelf", *J. Phys. Oceanography*, **18**, 724-737
- Haver, S. (2013), "Prediction of characteristic response for design purposes", Preliminary Revision 5, Statoil, Stavanger, Norway.
- Haver, S. (2016), "Stochastic description of ocean waves & response analysis and prediction of extremes", Lecture Note, Rev. 1, UIS/NTNU.
- Haver, S. and Nyhus, K.A. (1986), "A wave climate description for long term response calculations", OMAE, Tokyo.
- Kinsman, B. (1965), "Wind Waves", Englewood Cliffs, NJ: Prentice-Hall.
- Olagnon, M., Ewans, K., Forristall, G.Z. and Prevosto, M. (2013), "West Africa swell spectral shapes", *Proceedings of the Int. Conf. on Offshore Mech. and Arctic Eng.*, OMAE 2013-11228.
- Prevosto, M., Ewans, K., Forristall, G.Z. and Olagnon, M. (2013), "Swell genesis, modelling and measurements in West Africa", *Proceedings of the Int. Conf. on Offshore Mech. and Arctic Eng.*, OMAE 2013-11201.
- Sabique, L. (2012), "Effect of Southern swell on the waves in the Northern Indian Ocean swell propagation, effect and seasonal variability", Lambert Academic Publishing (2012-06-12).
- Sabique, L., Annapurnaiah, K., Nair Balakrishnan, T.M. and Srinivas, K. (2011), "Contribution of Southern Indian Ocean swells on the wave heights in the Northern Indian Ocean", A modeling study, *Ocean Eng.*, **43**, 113-120.
- Samiksha, S.V., Vethamony, P., Aboobacker, V. and Rashmi, R. (2012), "Propagation of Atlantic Ocean swells in the North Indian Ocean: A case study", *Natural Hazards and Earth System Sciences*, **12**, 3605-3615.
- Semedo, A., Sušelj, K. and Rutgersson, A. (2009), "Variability of wind sea and swell waves in the North Atlantic based on ERA-40 re-analysis", *Proceedings of the 8th European Wave and Tidal Energy Conference*, Uppsala, Sweden.
- Snodgrass, F.E., Groves, G.W., Hasselmann, K.F., Miller, G.R., Munk, W.H. and Powers, W.M. (1966), "Propagation of swell across the pacific", *Philos. T. R. Soc., London*, **259**, 431-497.

Appendix**Abbreviations**

CDF	Cummulative Density Function
DISTR	Distribution
DNV	Det Norske Veritas
DWR	Directional Waverider
FUPRE	University of Petroleum Resources
JONSWAP	Joint North Sea Wave Atmosphere Program
NCS	Norwegian Continental Shelf
NTNU	Norwegian University of Science and Technology
PM	Pierson and Moskowitz
UiS	University of Stavanger
WASP	West Africa Swell Project

Alphabetic symbols

H_s	Significant Wave Height
T_p	Peak wave period
T_z	Zero up-crossing wave period
F_{HS}	Cumulative Probability
h	Wave Height
h_s	Significant Wave Height
h_K	Sample significant wave height
n_{3h}	Number of 3-hour sample
$erfc$	Cumulative error Function
g_1	Sample Coefficient of Skewness
y_1	Probability Model Coefficient of Skewness
$\sigma_{H_s}^2$	Probability Model Variance
$s_{H_s}^2$	Sample Variance

Greek symbols

σ	Log-normal Location Parameter
β	3-parameter Weibull Shape Parameter
α	3-parameter Weibull Scale Parameter
μ	Log-normal Scale Parameter
k	Sample number
λ	3-parameter Weibull Location Parameter
Φ	Cumulative Standard Normal Distribution

